Vietnam Journal of Science and Technology ***63*** *(2) (2025) 388-401*
doi:10.15625/2525-2518/19286

Vabration analysis of continuous microbeams carrying a moving load

Pham Vu Nam[1], Vu Thi An Ninh[2], Nguyen Dinh Kien[3, 4, *]

[1]*Thuyloi University, 175 Tay Son, Dong Da, Ha Noi, Viet Nam*
[2]*University of Transport and Communications, 3 Cau Giay, Dong Da, Ha Noi, Viet Nam*
[3]*Institute of Mechanics, Vietnam Academy of Science and Technology, 18 Hoang Quoc Viet, Cau Giay, Ha Noi, Viet Nam*
[4]*VNU University of Engineering and Technology, 144 Xuan Thuy, Cau Giay, Ha Noi, Viet Nam*

[*]Email: *ndkien@imech.vast.vn*

Received: 27 October 2023; Accepted for publication: 6 March 2025

Abstract. Vibration analysis of continuous microbeams carrying a moving load is presented in the framework of the Euler-Bernoulli beam theory and the modified couple stress theory (MCST) for the first time. The continuous beams consist of three spans with nonuniform cross-section and simply supported ends. A finite element formulation is derived and used to establish the discretized equation of motion for the microbeams. Natural frequencies and dynamic response are determined with the aid of an implicit Newmark method. The derived formulation is validated by comparing the obtained results with data available in the literature. The numerical investigation reveals the importance of the microstructural size effect on the vibration of the continuous microbeams, and incorporating the material length scale parameter in the formulation leads to an increase in the vibration frequencies, but a decrease of the dynamic response. The effects of the material length scale parameter and moving load velocity on the vibration behavior of the continuous microbeams are studied in detail and highlighted.

Keywords: continuous microbeam, MCST, moving load, finite element formulation, vibration analysis.

Classification numbers: 5.4.2, 5.4.5.

1. INTRODUCTION

With wide application in practice, vibration of beam structures subjected to moving load has received much attention from researchers. Many reports on the dynamic response of one-span beam under a moving load can be found in the literature, e.g. Refs. [1 - 3]. Several investigations on vibration of continuous beams have been carried out, only the notable ones are shortly discussed herein. Henchi *et al.* [4] employed the dynamic stiffness method to predict dynamic response of three-span beam under a moving load. The analytical method and transfer-matrix method were used by Wang [5] to assess vibration characteristics of continuous Timoshenko beam with moving force. Zheng *et al.* [6] proposed the modified beam vibration functions containing cubic spline expressions as the assumed modes in their study on dynamic behavior of multi-span Timoshenko beams carrying a moving load.

Microbeams have been using extensively in microscopic devices such as microsensors, micro-electro mechanical systems (MEMs). Understanding the behavior of microbeams is crucial for design engineers. The traditional beam theories, however cannot predict the microstructural size effects due to the lack of material length scale parameter. Several higher-order continuum theories have been proposed, among which the modified couple stress theory (MCST) of Yang *et al.* [7] is widely adopted in modeling the microstructural size effect in microbeams. The dynamic analysis of Euler-Bernoulli beams under a moving microparticle was presented by Şimşek [8] in the framework of the MCST and the finite Fourier sine transformation, showing the importance of the material length scale parameter and the velocity of the microparticle on the dynamic behavior of the microbeam. The influence of microstructural effect on vibration of microbeams excited by a moving load/mass was investigated via the MCST by Jafari-Talookolaei *et al.* [9] using a semi analytical method, and by Esen *et al.* [10], Esen [11] using the finite element method.

The vibration analysis of microbeams discussed above are limited to single-span beams only. The use of intermediate supports is a common way in practice to reduce the dynamic magnification factor of beams. According to the authors' best knowledge, there is no study on vibration of continuous microbeams with two or more spans carrying a moving load so far. As an effort to narrow this gap, vibration analysis of a continuous microbeam under a moving load is presented in this work. A simply supported non-uniform three-span under a constant velocity moving load is considered herein. Due to the complexity of finding a closed-form solution satisfying boundary conditions at the multiple supports, analytical methods are hardly used in analyzing continuous beams, in general, vibration of continuous microbeams, in particular. The finite element method is adopted herein to study vibration of the three-span microbeam under a moving load. Energy expressions for the microbeam are derived in the framework of Euler-Bernoulli beam theory and the MCST. The equation of motion in discretized form for the microbeam is established by using a simple finite element formulation, and then solved by the Newmark direct integration method. The effects of the material length scale parameter and the velocity of the moving load on the vibration characteristics of continuous microbeam are examined and discussed in detail.

2. THEORY AND FORMULATION

Figure 1 shows a simply supported continuous microbeam with non uniform cross-section under a load P, moving with a constant velocity v from the left end to the right end of the beam. The beam consists of three spans with length of L, rectangular cross-section ($2b\times h$) for the middle span and ($b\times h$) for the two remaining spans. The x-axis of the Cartesian coordinate system in the figure is chosen on the microbeam mid-plane, and the z-axis directs upward. The investigation is carried out with an assumption that the moving load P is always in contact with the beam during its motion on the microbeam. In the figure, x_p is the current abscissa of the load P with respect to the left end of the continuous microbeam; A, B and C are midpoints of the first, second and third spans, respectively.

According to Euler-Bernoulli beam theory, the displacements $u_x(x,z,t)$ and $u_z(x,z,t)$ in the x and z directions, respectively, are given by

$$\begin{aligned} u_x(x,z,t) &= u(x,t) - zw_{,x}(x,t) \\ u_z(x,z,t) &= w(x,t) \end{aligned} \tag{1}$$

where $u(x,t)$ and $w(x,t)$ are the axial and transverse displacements of any point on the microbeam x-axis, respectively; t denotes the time variable. The subscript comma in Eq. (1), and hereafter, is used to denote the derivative with respect to the variable that follows.

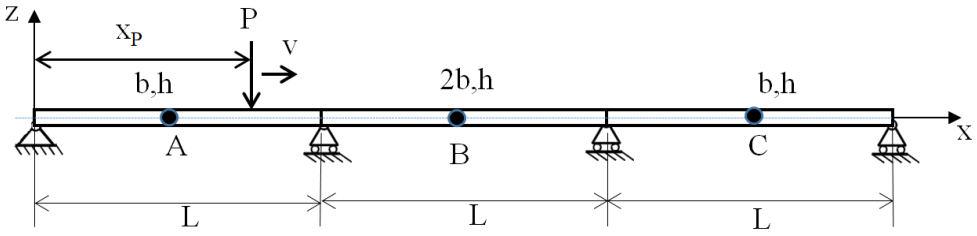

Figure 1. Three-span microbeam with non uniform cross-section under a moving load.

The microstructural size effect is modelled herein by using the modified couple stress theory of Yang *et al*. [10]. Accordingly, the strain energy U of the continuous microbeam is given by

$$U = \frac{1}{2}\int_V (\sigma_{ij}\varepsilon_{ij} + m_{ij}\chi_{ij})dV, \quad i,j = x,y,z \tag{2}$$

where V is the volume of the microbeam; σ_{ij} and ε_{ij} are, respectively, the components of the classical stress and strain tensors; m_{ij} and χ_{ij} refer to the components of the deviatoric part of the couple stress tensor and the curvature tensor, respectively. These components are defined as follows

$$\begin{aligned} \sigma_{ij} &= \lambda\varepsilon_{kk}\delta_{ij} + 2G\varepsilon_{ij}, \quad \varepsilon_{ij} = \frac{1}{2}(u_{i,j} + u_{j,i}) \\ m_{ij} &= 2l^2 G\chi_{ij}, \quad \chi_{ij} = \frac{1}{2}(\theta_{i,j} + \theta_{j,i}) \end{aligned} \tag{3}$$

where u_i ($I = x, y, z$) is the displacement in the i direction; l is the material length scale parameter measuring the effect of couple stress; δ_{ij} is the Kronecker delta; λ and G are Lame's constants which are related to the elastic modulus E and Poisson's ratio v as

$$\lambda = \frac{E\nu}{(1+\nu)(1-2\nu)}, \quad G = \frac{E}{2(1+\nu)} \tag{4}$$

with θ_i is component of the rotation vector and it's given by

$$\theta_i = \frac{1}{2}e_{ijk}u_{k,j} \tag{5}$$

where e_{ijk} represents the permutation symbol.

Using Eq. (1) and Eqs. (3) - (5), the strain energy of three-span continuous microbeam in Eq. (2) can be rewritten in the form

$$\begin{aligned} U &= \frac{1}{2}\sum_{k=1}^{3}\int_{(k-1)L}^{kL} (\sigma_{xx}\varepsilon_{xx} + 4l^2 G\chi_{xy}^2)\,dA_k \\ &= \frac{1}{2}\sum_{k=1}^{3}\int_{(k-1)L}^{kL} b_k h\left[(\lambda+2G)\left(u_{,x}^2 + \frac{h^2}{12}w_{,xx}^2\right) + l^2 G w_{,xx}^2\right]dx \end{aligned} \tag{6}$$

where b_k is the width of the ith span.

The kinetic energy T of the continuous microbeam is of the form

$$T = \frac{1}{2}\int_V \rho(\dot{u}_x^2 + \dot{u}_z^2)dV \tag{7}$$

where V is the volume of the microbeams; ρ is the mass density; the over dot indicates the partial derivative with respect to the time variable. From Eq. (1), the kinetic energy T can be rewritten in the form

$$T = \frac{1}{2}\sum_{k=1}^{3}\int_{(k-1)L}^{kL} \rho b_k h\left[(\dot{u}^2 + \dot{w}^2) + \frac{h^2}{12}\dot{w}_{,x}^2\right]dx \tag{8}$$

Finally, the potential energy V of the moving load P is given by

$$V = -\int_0^{3L} Pu_z\delta(x_P - vt)\,dx = -\int_0^{3L} Pw\delta(x_P - vt)\,dx \tag{9}$$

where $\delta(.)$ is the Dirac delta function.

By applying Hamilton's principle to Eqs. (6), (8) and (9) one can obtain the differential equations of motion for the continuous microbeam. However, finding a closed-form solution for such equations is cumbersome. In the next section, a finite element formulation is derived and used to establish the discretized equation of motion and to obtain the vibration characteristics of the continuous microbeam.

3. SOLUTION METHOD

Considering a two-node microbeam element with length l_e. The vector of nodal displacements **d** for the element contains six degrees of freedom as

$$\mathbf{d} = \{u_1 \quad w_1 \quad w_{,x1} \quad u_2 \quad w_2 \quad w_{,x2}\}^T \tag{10}$$

where u_i, w_i and $w_{,xi}$ (i = 1, 2) are the values of u, w and $w_{,x}$ at the node i. The superscript 'T' in Eq. (10) and hereafter is used to denote the transpose of a vector or a matrix.

The displacement field $\mathbf{u} = \{u \quad w\}^T$ in the each element is interpolated from the nodal values according to

$$\mathbf{u} = \mathbf{N}\mathbf{d} \tag{11}$$

where **N** are a shape function matrix of the following form

$$\mathbf{N} = \begin{bmatrix}\mathbf{N}_u \\ \mathbf{N}_w\end{bmatrix} = \begin{bmatrix} N_{u1} & 0 & 0 & N_{u2} & 0 & 0 \\ 0 & N_{w1} & N_{w2} & 0 & N_{w3} & N_{w4}\end{bmatrix} \tag{12}$$

In the Eq. (12), N_{ui} (i=1,2) are linear interpolation functions, N_{wi} (I = 1,…,4) are cubic Hermite polynomials.

Using the above interpolations, the strain energy of the beam in Eq. (6) can be written as

$$U = \frac{1}{2}\sum^{3nel}\mathbf{d}^T\mathbf{k}_e\mathbf{d} \tag{13}$$

where *nel* is the total number of elements used for each span, and $\mathbf{k}_e$ is the element stiffness matrix, and it is defined as follows

$$\mathbf{k}_e = \begin{cases} \int_0^{l_e} (\mathbf{N}_{u,x}^T A_1 \mathbf{N}_{u,x} + \mathbf{N}_{w,xx}^T B_1 \mathbf{N}_{w,xx}) dx & \text{for the first span} \\ \int_0^{l_e} (\mathbf{N}_{u,x}^T A_2 \mathbf{N}_{u,x} + \mathbf{N}_{w,xx}^T B_2 \mathbf{N}_{w,xx}) dx & \text{for the second span} \\ \int_0^{l_e} (\mathbf{N}_{u,x}^T A_3 \mathbf{N}_{u,x} + \mathbf{N}_{w,xx}^T B_3 \mathbf{N}_{w,xx}) dx & \text{for the third span} \end{cases} \tag{14}$$

where

$$A_i = b_i h(\lambda + 2G), \quad B_i = \frac{b_i h^3}{12}(\lambda + 2G) + b_i h l^2 G, \qquad i = 1,2,3 \tag{15}$$

Similarly, the kinetic energy of the beam in Eq (8) can be written in the following form

$$T = \frac{1}{2}\sum^{3nel} \dot{\mathbf{d}}^T \mathbf{m}_e \dot{\mathbf{d}} \tag{16}$$

where the element mass matrix $\boldsymbol{m}_e$ of the beam is defined as

$$\mathbf{m}_e = \begin{cases} \int_0^{l_e} (\mathbf{N}_u^T C_1 \mathbf{N}_u + \mathbf{N}_w^T C_1 \mathbf{N}_w + \mathbf{N}_{w,x}^T D_1 \mathbf{N}_{w,x}) dx & \text{for the first span} \\ \int_0^{l_e} (\mathbf{N}_u^T C_2 \mathbf{N}_u + \mathbf{N}_w^T C_2 \mathbf{N}_w + \mathbf{N}_{w,x}^T D_2 \mathbf{N}_{w,x}) dx & \text{for the second span} \\ \int_0^{l_e} (\mathbf{N}_u^T C_3 \mathbf{N}_u + \mathbf{N}_w^T C_3 \mathbf{N}_w + \mathbf{N}_{w,x}^T D_3 \mathbf{N}_{w,x}) dx & \text{for the third span} \end{cases} \tag{17}$$

with

$$C_i = \rho b_i h, \quad D_i = \rho \frac{b_i h^3}{12}, \qquad i = 1,2,3 \tag{18}$$

The potential energy in Eq. (9) is of the form

$$V = -\sum^{3nel} \mathbf{d}^T \mathbf{f}_P \tag{19}$$

where $\mathbf{f}_P$ is the time-dependent element nodal load vector generated by the moving load *P*, and it has the form

$$\mathbf{f}_P = P\,\mathbf{N}_w^T\Big|_{x_e} \tag{20}$$

where x_e is the current abscissa of the moving load *P* with respect to the left node of the element.

The discretized equation of motion for the continuous microbeam under a moving load in case of neglecting the damping effect can be written in the following form

$$\mathbf{M}\ddot{\mathbf{D}} + \mathbf{K}\mathbf{D} = \mathbf{F} \tag{21}$$

where $\mathbf{D}$ and $\ddot{\mathbf{D}}$ are, respectively, the global vectors of nodal displacements and accelerations; $\mathbf{M}$ and $\mathbf{K}$ are, respectively, the structural mass and stiffness matrices, constructed by merging the derived element mass and stiffness matrices over the total number of elements. $\mathbf{F}$ is the global

vector constructed by assembling $\mathbf{f}_P$ over the elements. Equation (21) can be solved by a direct integration Newmark method. The average acceleration method that ensures the unconditional convergence of the numerical solution is adopted herein.

4. NUMERICAL INVESTIGATION

In this section, the vibration of the simply supported three-span continuous microbeam subjected to a moving load is investigated numerically. A microbeam made from steel (SUS304) with E = 210 GPa, ρ = 7800 kg/m^3, ν = 0.3 [12] is considered. The parameters of the microbeam used for calculation are as follows: h = 10 μm, $b_2 = 2b_1 = 2b_3 = 2$ μm, and an aspect ratio L/h = 20.

For convenience, the non-dimension parameters μ_i, f_v, η, D_d(A), D_d(B) and D_d(C) are introduced, respectively, for the natural frequencies, moving load velocity, material length scale parameter and dynamic magnification factor at the positions A, B, C as [12]

$$\mu_i = \omega_i L_B \sqrt{\frac{\rho(1+\nu)(1-2\nu)}{E(1-\nu)}}, \quad f_v = \frac{\pi v}{\omega_1 L_B}, \quad \eta = \frac{l}{h},$$
$$\mathrm{D}_d(\mathrm{A}) = \max\left[\frac{w(L/2,t)}{w_{st}}\right], \mathrm{D}_d(B) = \max\left[\frac{w(3L/2,t)}{w_{st}}\right], \mathrm{D}_d(C) = \max\left[\frac{w(5L/2,t)}{w_{st}}\right] \tag{22}$$

where ω_i is the ith natural frequency; L_B=3L is the total length of the continuous microbeam; $w_{st} = PL_B^3 / 48EI_2$ is the static deflection of the single-span steel beam with the moment of inertia $I_2 = b_2 h^3 / 12$ under a load P at the mid-span.

Table 1. Convergence study and validation for fundamental frequency parameters of a single-span microbeam (η = 0.5, L/h =10).

Material	*Nel* = 2	*Nel* = 4	*Nel* = 6	*Nel* = 8	*Nel* = 10	Ref. [13]
Al	0.3882	0.3868	0.3867	0.3867	0.3867	0.3863
SiC	0.8691	0.8660	0.8658	0.8657	0.8657	0.8538

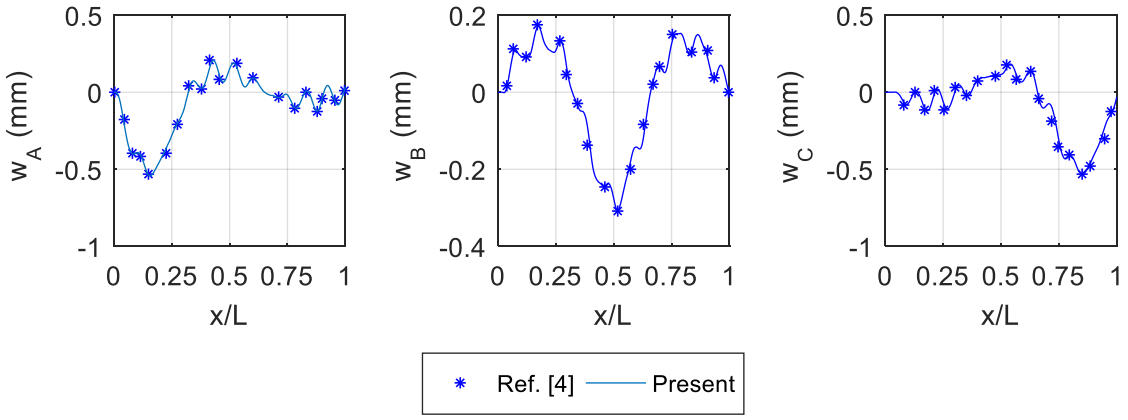

Figure 2. Comparison of dynamic vertical deflection at the midpoint of each span of continuous marcrobeam (η = 0) with the positions of moving load.

The accuracy and convergence of the proposed beam element are firstly confirmed. To this purpose, in Table 1, the convergence and validation in evaluating the fundamental frequency parameters are presented for single-span microbeam. The results in Table 1 are given for microbeam made from aluminium (Al) and black silicon carbide (SiC).

It is observed that the convergence of beam element is achieved by using only ten elements. For the validation purpose, the frequency parameters obtained in present work agree very well with that of Ansari *et al.* [13] where the Navier solution form is used.

In Figure 2, the relations between the dynamic deflections of a continuous marcrobeam (η = 0) with the position of the moving load obtained in this paper are compared with that of Henchi *el al*. [4]. In the figure, points A, B and C are the midpoints of the first, second and third spans, respectively. As can be noted from Figure 2 that a good agreement between the results of the present work with the results using dynamic finite element model of Henchi *el al*. [4] is obtained.

The convergence of the derived beam element in evaluating the dynamic magnification factor at positions A, B and C of the three-span continuous microbeam is shown in Table 2 for L/h = 20, η = 0.2, f_v = 0.05. As observed from this table, the convergence of the derived element is also achieved using ten elements for each span. Because of this convergence result, ten elements/span are used for all the computations reported below.

Table 2. Convergence of the microbeam element in evaluating dynamic magnification factors at the midpoint of each span for L/h = 20, η = 0.2, f_v = 0.05.

	Nel = 2	*Nel* = 4	*Nel* = 6	*Nel* = 8	*Nel* = 10
D_d(A)	0.0306	0.0305	0.0304	0.0304	0.0304
D_d(B)	0.0177	0.0178	0.0178	0.0178	0.0178
D_d(C)	0.0311	0.0305	0.0304	0.0305	0.0305

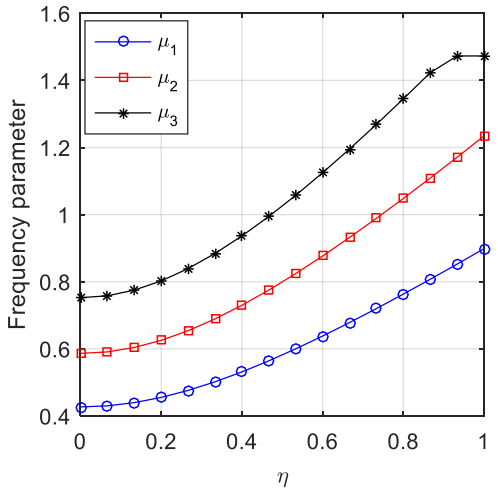

Figure 3. Variation of the first three frequency parameters of continuous microbeam with parameter η.

The influence of the dimensionless material length scale parameter η on the natural frequencies of the three-span continuous microbeam is shown in Figure 3, where the variation of the first three frequency parameters with the dimensionless scale parameter η are depicted. One can see from the figure that the frequency parameters obtained from traditional beam theory (η = 0) are always lower than that calculated from the MCST. This can be explained by observing Eq. (6), where the presence of the parameter η in the MCST leads to an increase of the microbeam stiffness. Besides, an increase in the parameter η results in an increase in the frequency parameter, and this is correct for all the three frequency parameters considered herein.

The dynamic magnification factors at positions A, B and C of the three-span microbeam are presented in Table 3 for a velocity parameter f_v = 0.1 and different values of the dimensionless material length scale parameter (η = 0, 0.1, 0.25, 0.5, 0.75, 1). It is clear from Table 3 that the effect of the parameter η on the dynamic magnification factor is significant, and increasing the parameter η leads to a sharp decrease in the dynamic magnification factor, regardless of considered point (A, B or C). On the other hand, the factor D_d at the points A, B, C obtained by using the MCST is always lower than that using the conventional beam theory. Observing from Table 3 as well as Figure 4 one can see that when a moving load moves on the beam, the values of the factors D_d(A) and D_d(C) are close to each other while the factor D_d(B) is always the lowest, regardless of the parameter η. This result can be explained by the fact that the width of the cross-section of the second span considered in this paper is twice wider than that of the first and the third spans. As a result, the bending stiffness of the second span is also twice larger than that of the first span and the third span.

Table 3. Dynamic magnification factor of continuous microbeam under a moving load (f_v = 0.1).

η	*Dd*(A)	*Dd*(B)	*Dd*(C)
0	0.0403	0.0221	0.0361
0.1	0.0389	0.0214	0.0349
0.25	0.0332	0.0182	0.0298
0.5	0.0217	0.0119	0.0195
0.75	0.0137	0.0076	0.0123
1	0.0091	0.0050	0.0081

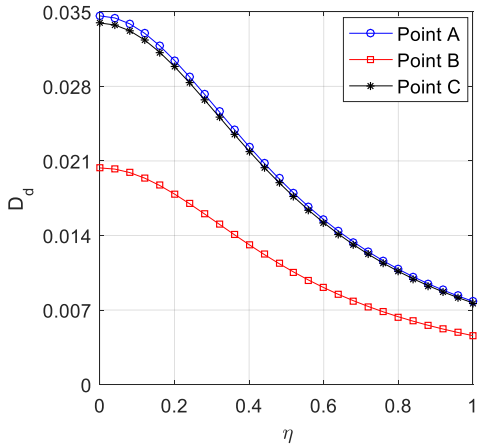

Figure 4. Variation of dynamic magnification factor at A, B and C with the parameter η (f_v = 0.05).

The time histories for deflection at the points A, B and C of the continuous microbeam are respectively presented in Figures 5 - 7 for various values of the length scale parameter η and the velocity parameter f_v. In the figures, ΔT is the total time necessary for the load P crossing the microbeam. Several remarks can be drawn from observation of these figures.

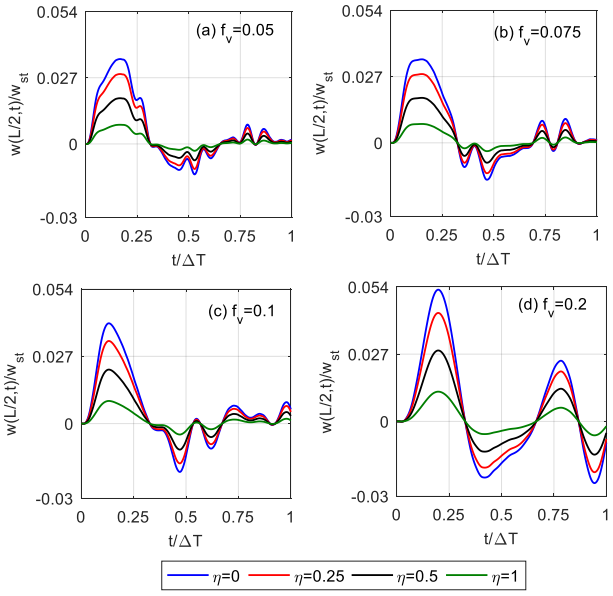

Figure 5. Time histories for deflection at point A with different values of the parameter η.

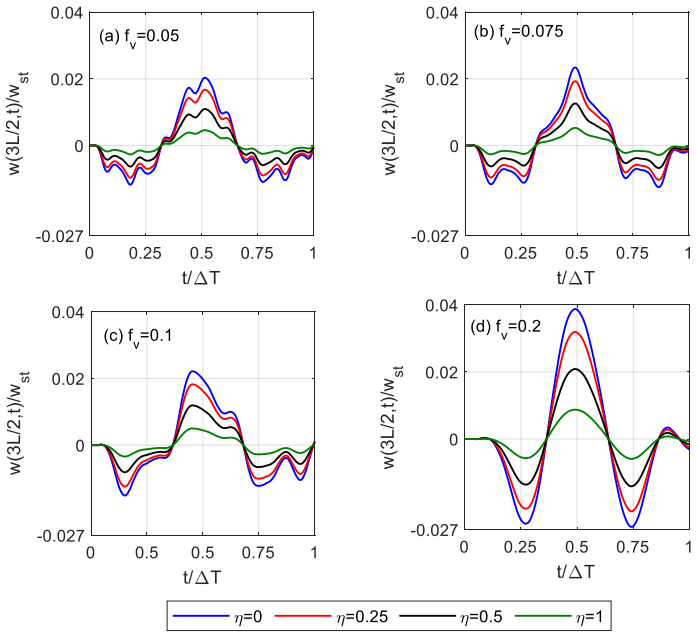

Figure 6. Time histories for deflection at point B with different values of the parameter η.

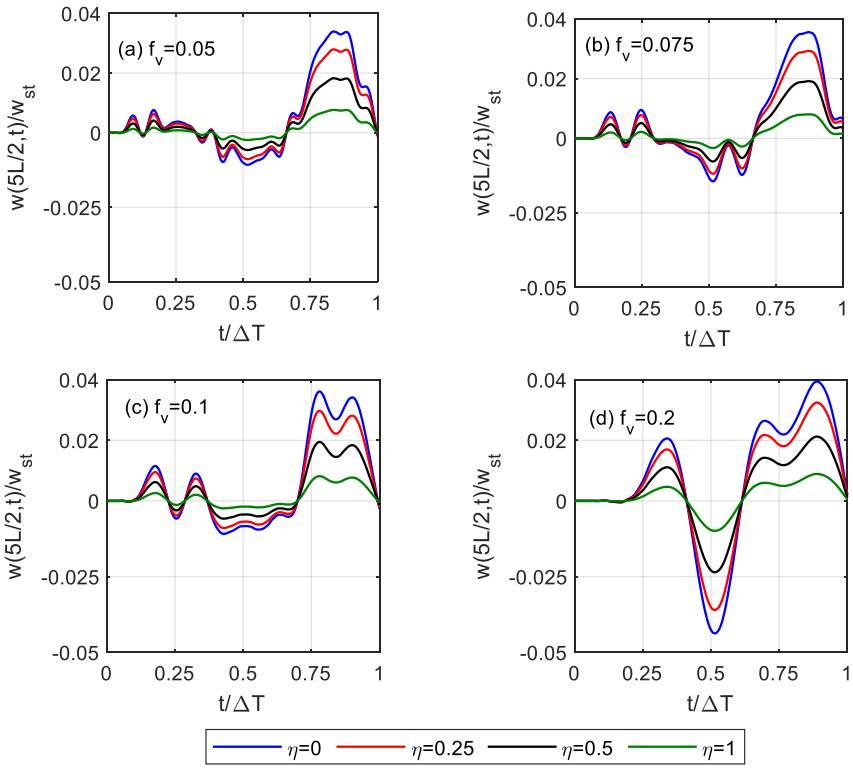

Figure 7. Time histories for deflection at point C with different values of the parameter η.

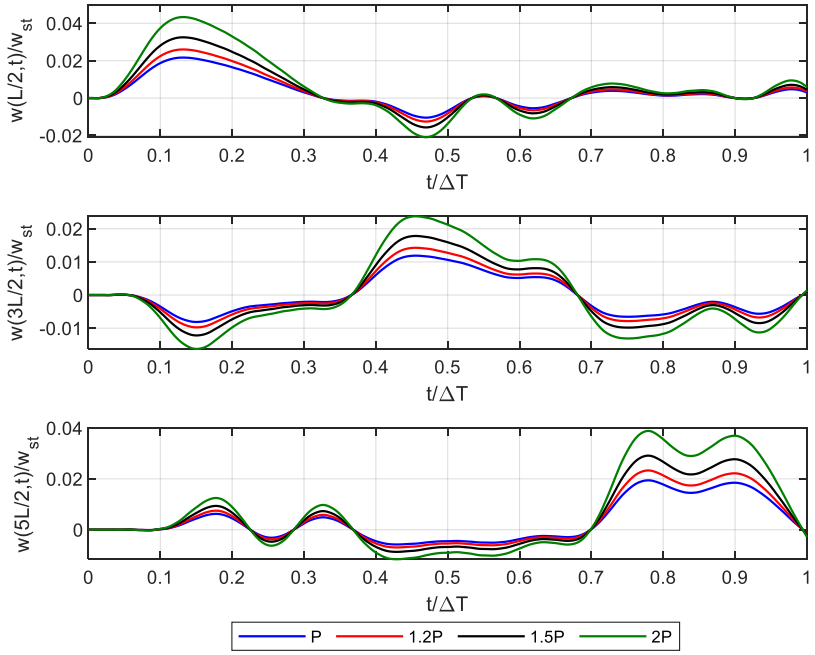

Figure 8. Time histories for deflection at the points A, B and C with different values of moving load (η = 0.5, f_v = 0.1).

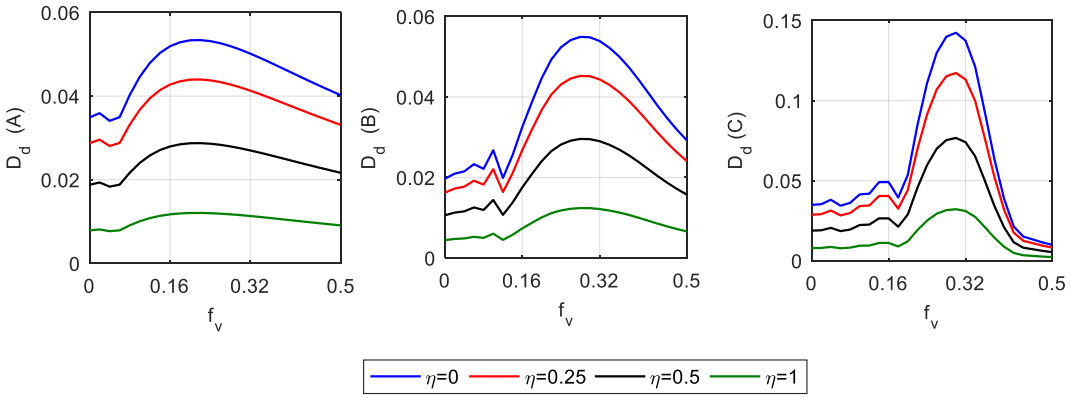

Figure 9. Variation of dynamic magnification factor at points A, B and C with the velocity parameter for the different values of parameter η.

Firstly, the influence of the size effect is confirmed again from the figures, where the deflection amplitude is decreased by increasing the scale parameter η, regardless of the load velocity and the considered point. Secondary, the moving load velocity plays an important role on the vibration of the microbeam, and both the deflection and the way the microbeam vibrates are significantly affected by the load velocity.

The maximum deflection at the mid points tends to increase for a higher velocity, regardless of the scale parameter η. The microbeam executes less vibration modes when the load velocity is high, and this phenomenon is correct for all three points, regardless of the scale parameter. In addition, the scale parameter just alters the vibration amplitute, and it hardly changes the way the microbeam vibrates. Figure 8 presents the time histories at the points A, B and C for η = 0.5, f_v = 0.1 and different movings. The change of the moving load amplitude, as seen from the figures, alters the time histories at the considered points significantly, and as expected, the dynamic deflection of the microbeam is higher when it is subjected to a larger moving load.

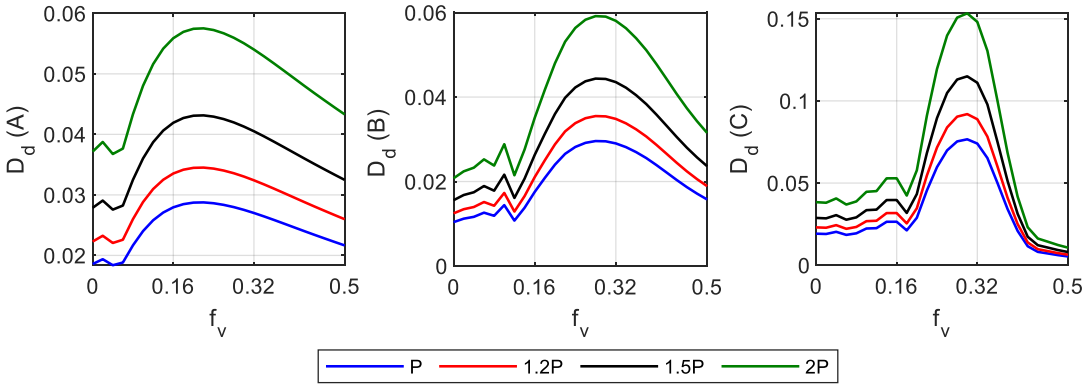

Figure 10 . Variation of dynamic magnification factor at points A, B and C with the velocity parameter for the different values of moving load (η = 0.5).

The effects of the scale parameter and the moving load amplitude on the dynamics of the continuous microbeam are shown in Figures 9 and 10, where the variation of the dynamic magnification factor at the midpoint of each span with the velocity parameter f_v are depicted for different values of the parameter η and the load P, respectively. As seen from the figures, the dynamic magnification factors repeatedly increase and decrease when prarameter f_v increases, then they reach the maximum values. Furthermore, the maximum dynamic magnification factor at point A attains at the earliest time, while it is the latest for the point C. Besides, the maximum dynamic magnification factor obtained at point C is always higher than that obtained at points A and B, regardless of the value of the scale parameter η and moving load amplitude. The relation between the dynamic magnification factor at the midpoint of each span and the velocity parameter is highly dependent on the parameter η and the moving load amplitude. The dynamic factor is decreased by the increase of the scale parameter η, as can be observed from Fig. 9, and as expected, it is increased by the increase of the moving load, as can be seen in Fig. 10.

The maximum axial stresses at the mid-span sections are presented in Table 4 for $f_v = 0.05$ and different material length scale parameters and the load positions. The ãial stress σ_{xx} in the table is normalized by $\sigma_0 = P/(b_1 h)$, and at the time when the moving load arrives at the points A, B and C. As expected, the maximum stress decreases when parameter η increases, regardless of the load position and considered section. It is observed from the table that when the moving load arives at any midpoint, the maximum stress obtained at that section is the largest, regardless of the dimensionless material length scale parameter η.

Table 4. Maximum axial stresses at mid-span sections for different material length scale parameters and load positions ($f_v = 0.05$).

Load position	Section	η					
		0	0.1	0.25	0.5	0.75	1
P at A	A	22.5638	21.8158	18.5820	12.1497	7.7047	5.0951
	B	3.9380	3.8074	3.2430	2.1204	1.3447	0.8892
	C	3.3298	3.2194	2.7422	1.7930	1.1370	0.7519
P at B	A	2.2444	2.1700	1.8483	1.2086	0.7664	0.5068
	B	12.2836	11.8765	10.1159	6.6143	4.1944	2.7737
	C	3.7610	3.6364	3.0973	2.0252	1.2843	0.8493
P at C	A	0.2677	0.2590	0.2205	0.1443	0.0915	0.0605
	B	2.1644	2.0927	1.7825	1.1654	0.7391	0.4887
	C	22.5697	21.8215	18.5868	12.1529	7.7067	5.0964

5. CONCLUSIONS

Vibration analysis of a continuous microbeam carrying a moving load has been presented. The three-span microbeam with nonuniform cross-section is considered. A size-dependent finite element formulation was derived on the basis of Euler-Bernoulli and the MSCT, and used to establish the discretized motion equation for the continuous microbeam. Vibration characteristics were computed using the Newmark method. The effects of the scale parameter and the velocity parameter of the moving load on the vibration of the microbeam have been

studied in detail. The most important points from the results obtained in the present work can be summarized as follows.

- The results obtained from the derived formulation of this present work agree well with the results previously published in the literature.
- The size scale parameter plays an important role on the vibration of the microbeam. The frequency parameters obtained from traditional beam theory are always lower than that calculated from the MSCT. An increase in the material length scale parameter η leads to an increase in the frequency parameters and a decrease in the dynamic magnification factor.
- The deflection at the midpoint of each span is significantly affected by the velocity parameter, the maximum deflection as well as the way the microbeam vibrates.

Acknowledgements. The work presented in this article was supported by Vietnam Academy of Science and Technology (VAST), Grant number CT0000.01/23-24.

CRediT authorship contribution statement. Pham Vu Nam: Data curation, Formal analysis, Investigation. Vu Thi An Ninh*:* Software, Validation, Investigation, Writing - original draft. Nguyen Dinh Kien: Supervision, Methodology, Funding acquisition, Review & editing.

Declaration of competing interest. The authors declare that they have no known competing financial interests or personal relationships that could have appeared to influence the work reported in this paper.

REFERENCES

1. Kargarnovin M. H., Younesian D. - Dynamics of Timoshenko beams on Pasternak foundation under moving load, Mechanics research communications **31** (6) (2004) 713-723. https://doi.org/10.1016/j.mechrescom.2004.05.002.
2. Uzzal R. U. A., Bhat R. B., Ahmed W. - Dynamic response of a beam subjected to moving load and moving mass supported by Pasternak foundation, Shock and Vibration **19** (2) (2012) 201-216. DOI: 10.3233/SAV-2011-0624.
3. Yang Y., Ding H. Chen L. Q. - Dynamic response to a moving load of a Timoshenko beam resting on a nonlinear viscoelastic foundation, Acta Mechanica Sinica **29** (5) (2013) 718-727. https://doi.org/10.1007/s10409-013-0069-3.
4. Henchi K., Fafard M., Dhatt G., Talbot M. - Dynamic behaviour of multi-span beams under moving loads, Journal of sound and vibration **199** (1) (1997) 33-50. https://doi.org/10.1006/jsvi.1996.0628.
5. Wang R. T. - Vibration of multi-span Timoshenko beams to a moving force, Journal of sound and vibration **207** (5) (1997) 731-742. https://doi.org/10.1006/jsvi.1997.1188.
6. Zheng D. Y., Cheung Y. K., Au F. T. K., Cheng Y. S. - Vibration of multi-span non-uniform beams under moving loads by using modified beam vibration functions, Journal of Sound and vibration **212** (3) (1998) 455-467. https://doi.org/10.1006/jsvi.1997.1435
7. Yang F. A. C. M., Chong A. C. M., Lam D. C. C., Tong P. - Couple stress based strain gradient theory for elasticity, International journal of solids and structures **39** (10) (2002) 2731-2743. https://doi.org/10.1016/S0020-7683(02)00152-X.
8. Şimşek M. - Dynamic analysis of an embedded microbeam carrying a moving microparticle based on the modified couple stress theory, International Journal of

Engineering Science **48** (12) (2010) 1721-1732. https://doi.org/10.1016/j.ijengsci.2010.09.027.

9. Jafari-Talookolaei R. A., Abedi M., Şimşek M., Attar M. - Dynamics of a micro scale Timoshenko beam subjected to a moving micro particle based on the modified couple stress theory, Journal of Vibration and Control **24** (3) (2016) 527-548. https://doi.org/10.1177/1077546316645237.
10. Esen I., Abdelrahman A. A., Eltaher M. A. - Dynamics analysis of timoshenko perforated microbeams under moving loads, Engineering with Computers (2020) 1-17. https://doi.org/10.1007/s00366-020-01212-7.
11. Esen I. - Dynamics of size-dependant Timoshenko micro beams subjected to moving loads, International Journal of Mechanical Sciences **175** (2020), 105501. https://doi.org/10.1016/j.ijmecsci.2020.105501.
12. Zhang Q., Liu H. - On the dynamic response of porous functionally graded microbeam under moving load, International Journal of Engineering Science **153** (2020) 103317. https://doi.org/10.1016/j.ijengsci.2020.103317.
13. Ansari R., Gholami R., Sahmani S. - Free vibration analysis of size-dependent functionally graded microbeams based on the strain gradient Timoshenko beam theory, Composite Structures **94** (1) (2011) 221-228. https://doi.org/10.1016/j.compstruct.2011.06.024